Electronic Supplementary Material (ESI) for Dalton Transactions.

Supporting Information

Trivalent Copper Stabilised by Acetylacetone Dithiocarbazate Schiff Base Ligands: structural, spectroscopic and electrochemical properties.

Jessica K. Bilyj, Nicole V. Silajew, Graeme R. Hanson, Jeffrey R. Harmer and Paul V. Bernhardt

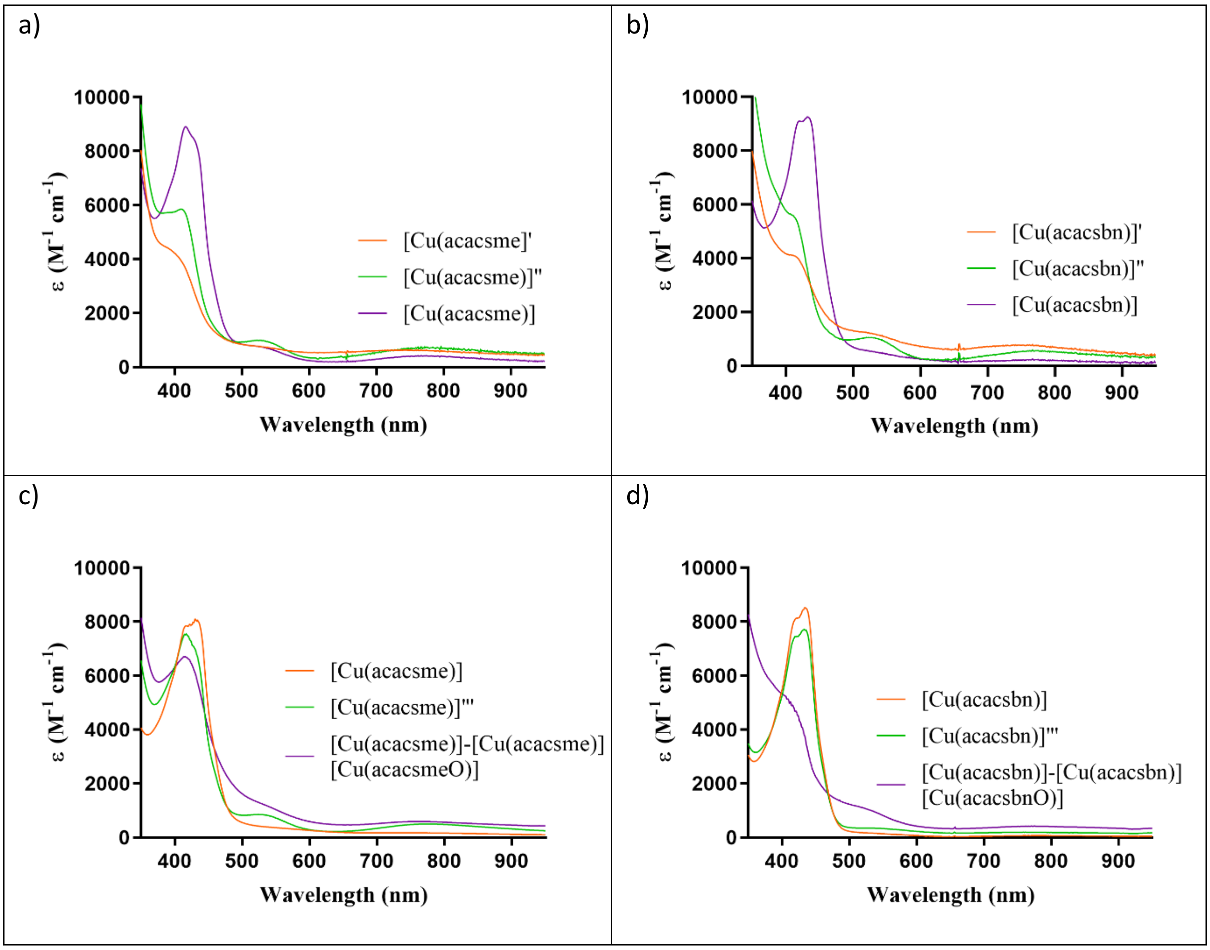

Figure S1. Reactlab Kinetics calculated spectra of a) [Cu^{II}(Hacacsme)] formation (anaerobic) b) [Cu^{II}(Hacacsbn)] formation (anaerobic) c) the oxidation of [Cu^{II}(Hacacsme)] to give [Cu^{II}(acacsmeO)] and [(Cu^{III}(acacsme))$_2$] and d) oxidation of [Cu^{II}(Hacacsbn)] to give [Cu^{II}(acacsbnO)] and [(Cu^{III}(acacsbn))$_2$].

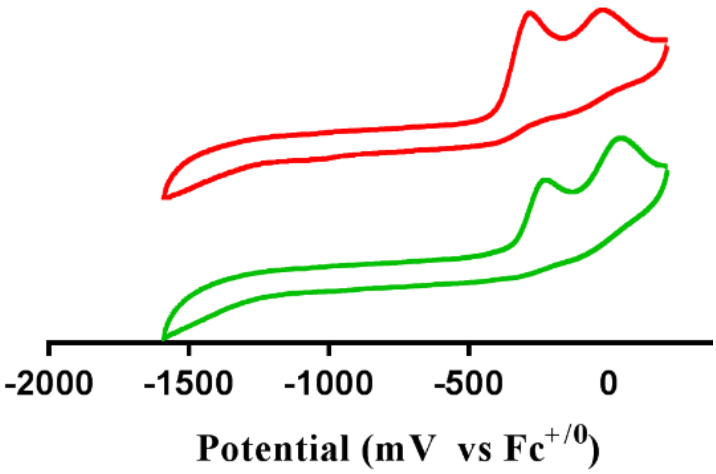

Figure S2. Cyclic voltammograms of H_3acacsme (red) and H_3acacsbz (green) in DMF with 0.1 M Et_4NClO_4 at 200 mV/s sweep rate.

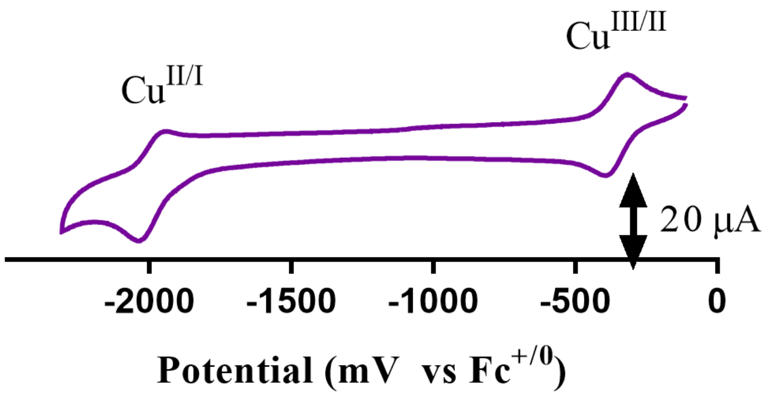

Figure S3. Cyclic voltammetry of crystalline [Cu^{III}(acasme)] (2.7 mM in DMF and 0.1 M Et_4NClO_4) at a sweep rate of 500 mV/s.

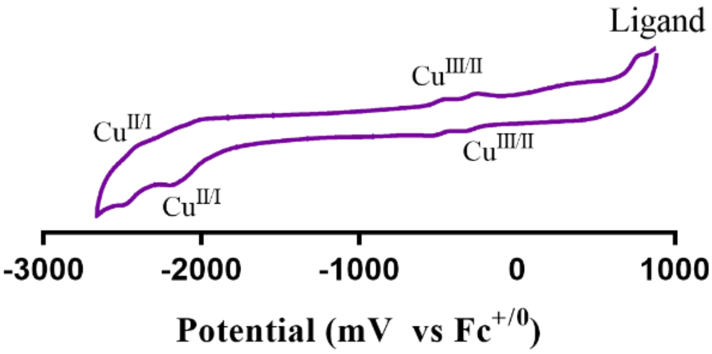

Figure S4. Cyclic voltammetry of crystalline [(Cu^{III}(acasbn))$_2$] (in DMF and 0.1 M Et_4NClO_4) at a sweep rate of 500 mV/s. Working electrode glassy carbon.

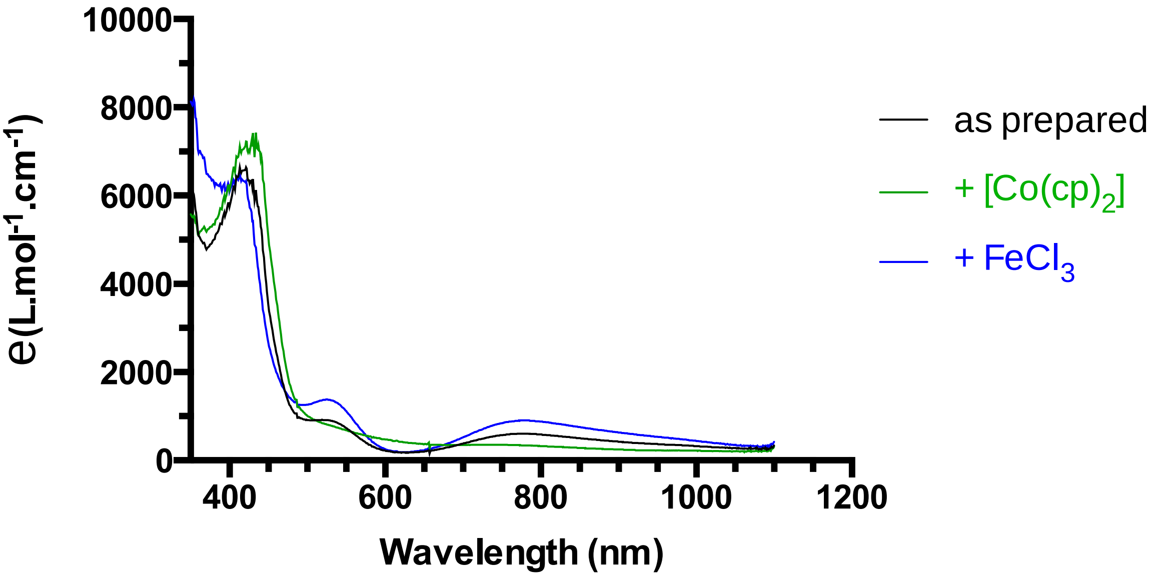

Figure S5. UV-Vis spectra of [Cu^{III}(acacsme)] (black) as prepared (partially reduced by the DMF solvent) (0.136 mM in DMF); [Cu^{III}(acacsme)] reduced with cobaltocene to its monoanion [Cu^{II}(acacsme)]$^{-}$ (green); [Cu^{III}(acacsme)] oxidised with $FeCl_3$ (blue). Cobaltocene and $FeCl_3$ have negligible absorbance in these regions.

a)

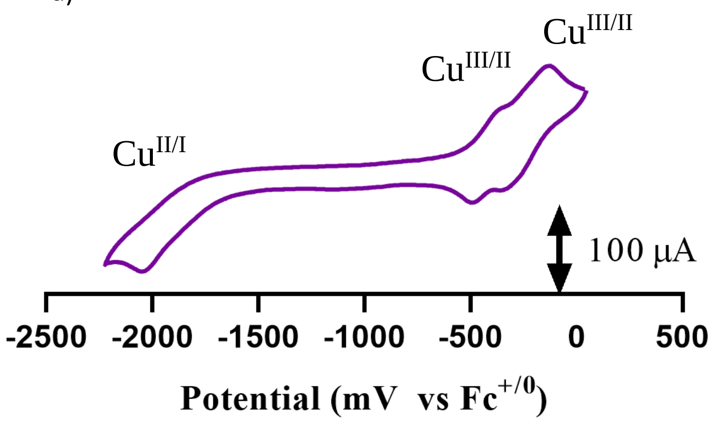

b)

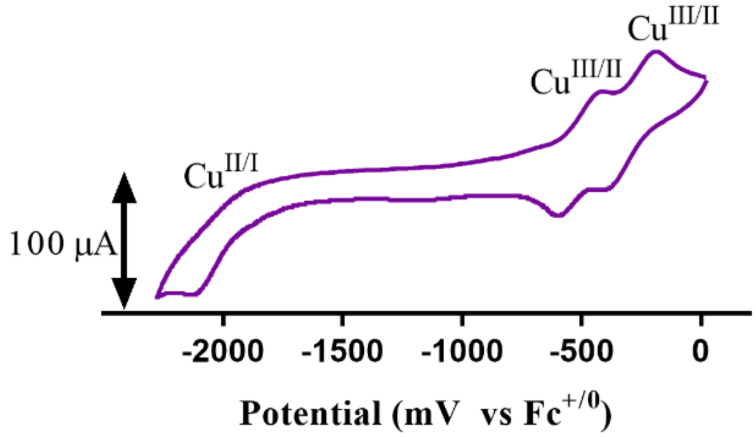

Figure S6 CVs of the dimeric complexes a) [(Cu(acacsme)$_2$)] and b) [(Cu(acacsbn)$_2$)] formed *in situ* from aerial oxidation of their [Cu(HacacsR)] precursors in the presence of excess Et_3N. Scan rate 200 mV s^{-1} DMF and 0.1 M Et_4NClO_4.

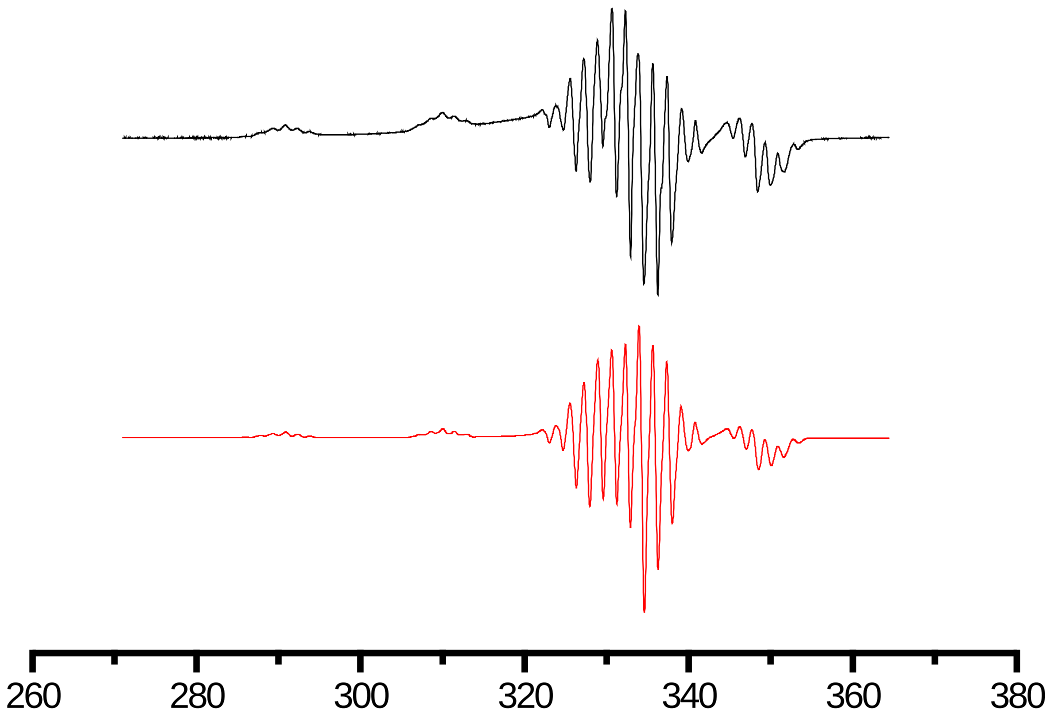

Figure S7. Experimental (top) and simulated (bottom) X-band CW EPR spectra of $[Cu^{II}(acacsme)]^{-}$ (1.36 mM in DMF, ν = 9.430 GHz, 140 K). Spin Hamiltonian parameters: g_x 2.0261 ($A_{x,Cu}$ 36.6 × 10^{-4}, $A_{x,N}$ 15.7 × 10^{-4} cm^{-1}); g_y 2.0266 ($A_{y,Cu}$ 36.6 × 10^{-4}, $A_{y,N}$ 16.2 × 10^{-4} cm^{-1}); g_z 2.1072 ($A_{z,Cu}$ 188.5 × 10^{-4}, $A_{z,N}$ 14.2 × 10^{-4} cm^{-1}).

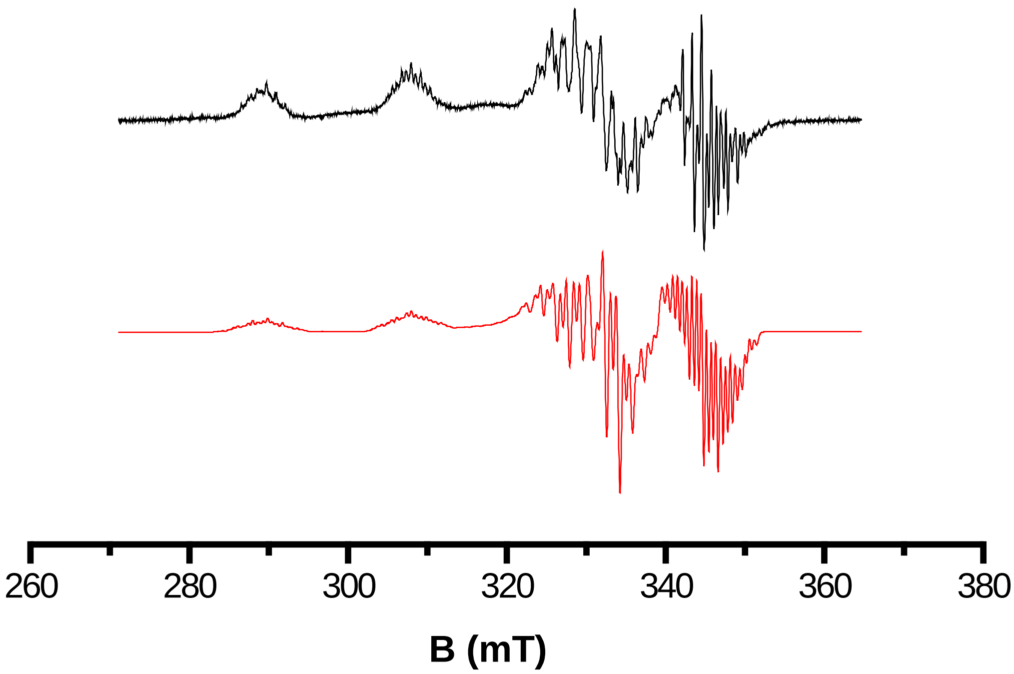

Figure S8. Experimental (top) and simulated (bottom) X-band CW EPR spectra of crystalline [Cu^{II}(acacsmeO)] (0.65 mM in DMF, ν =9.432 GHz, 140 K). Spin Hamiltonian parameters: g_x 2.0254 ($A_{x,Cu}$ 37.0 × 10^{-4}, $A_{x,N}$ 17.7 × 10^{-4} cm^{-1}); g_y 2.0279 ($A_{y,Cu}$ 36.5 × 10^{-4}, $A_{y,N}$ 14.6 × 10^{-4} cm^{-1}); g_z 2.1250 ($A_{z,Cu}$ 180.0 × 10^{-4}, $A_{z,N}$ 18.5 × 10^{-4} cm^{-1}).

a) [Cu(Hacacsbn)] + O_2 → [Cu^{II}(acacsbnO)] (major) + [(Cu(acacsbn))$_2$] (*)

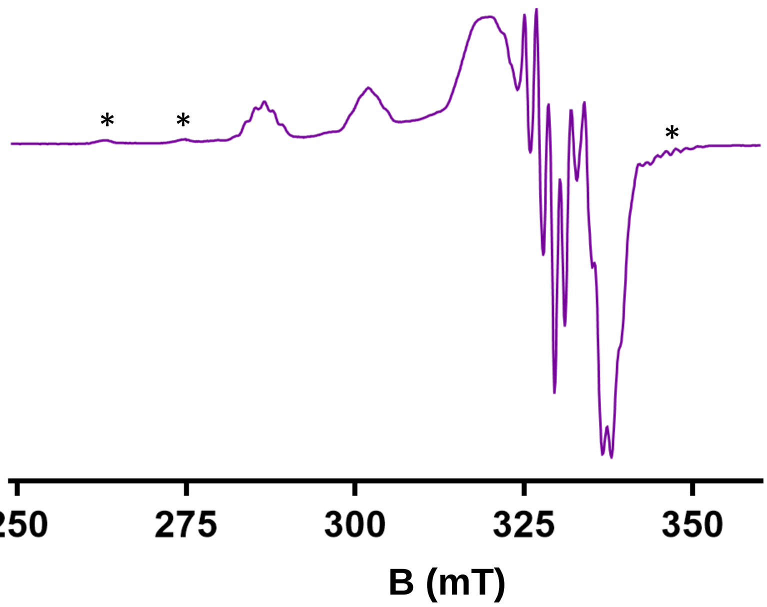

b) [Cu(Hacacsbn)] + O_2 + Et_3N → [(Cu(acacsbn))$_2$] (major)

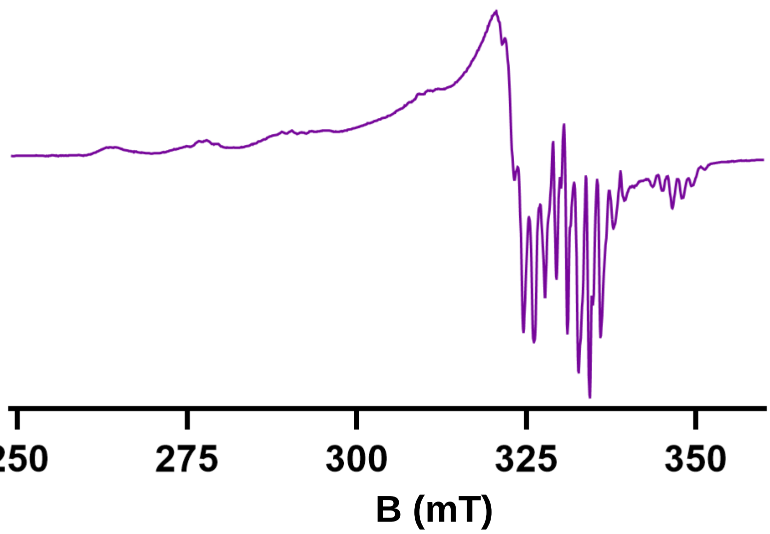

c) [(Cu(acacsbn))$_2$] crystals

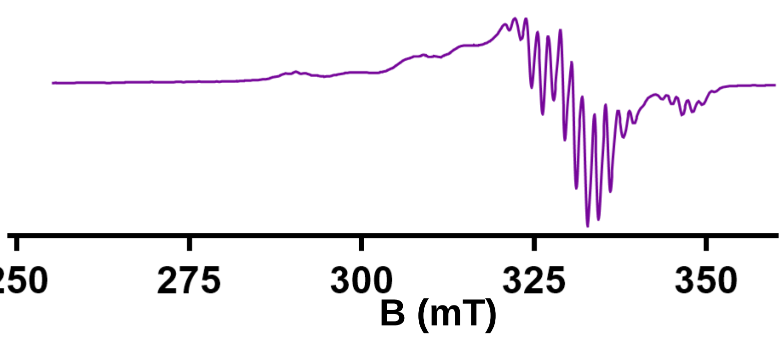

Figure S9. X-band CW EPR spectra (ν = 9.3742 GHz) of frozen DMF solutions (130 K) of a) [Cu^{II}(acacsbnO)] and minor amounts of reduced dimer (*) produced aerobically without added base b) the same solution prepared aerobically with added Et_3N c) crystalline dimer [(Cu(acacsbn))$_2$].